Phys. Chem. Minerals 4, 43–53 (1979)

PHYSICS AND CHEMISTRY OF MINERALS

Determination of Quantitative Cation Distribution in Orthopyroxenes From Electronic Absorption Spectra

Don S. Goldman[1] and George R. Rossman[2]

[1] Technical Center, Owens/Corning Fiberglas Corporation, Granville, Ohio 43023, USA
[2] Division of Geological and Planetary Sciences, California Institute of Technology, Pasadena, California 91125, USA*

Abstract. Electronic and Mössbauer absorption spectra and electron microprobe data are correlated for iron-bearing orthopyroxenes. The correlation provides a means of quantitatively determining the distribution of Fe^{2+} between the $M(1)$ and $M(2)$ sites of orthopyroxene crystals from electronic spectra and electron microprobe analysis. The electronic spectra are used to analyze the changes in the Fe^{2+} distribution produced during heating experiments and confirm earlier results from Mössbauer spectra. Two components of the spin-allowed transition of Fe^{2+} in the $M(1)$ site are identified at about 13,000 cm^{-1} and 8,500 cm^{-1} in γ. Molar absorptivity (ε) values for all spin-allowed Fe^{2+} absorption bands in the near-infrared region are determined. The $M(2)$ Fe^{2+} band at $\sim$5,000 cm^{-1} in β is the analytically most useful for site occupancy determinations. It remains linear with concentration ($\varepsilon = 9.65$) over the entire compositional range. The band at $\sim$10,500 cm^{-1} in α is the most sensitive to $M(2)$ Fe^{2+} concentration ($\varepsilon = 40.8$), but deviates from linearity at high iron concentrations. The origins of spin-forbidden transitions in the visible region are examined.

Introduction

The distribution of ferrous iron between the two non-equivalent six-coordinate sites in orthopyroxene, $(Mg, Fe)SiO_3$, has been extensively analyzed, using Mössbauer spectroscopy and X-ray structural refinements, because of its potential applications in geothermometry. Ghose (1965) found that Fe^{2+} preferentially occupies the large, highly-distorted $M(2)$ site. Evans et al. (1967) observed that the distribution of Fe^{2+} between the $M(1)$ and $M(2)$ sites is dependent upon temperature. Ghose and Hafner (1967) showed that Fe^{2+} is more strongly partitioned into the $M(2)$ site in slowly cooled metamorphic rocks than in quickly cooled volcanic rocks. These observations suggested that the cation distribution

* Contribution No. 3058

0342-1791/79/0004/0043/$02.20

depends on the rate of cooling, which led Virgo and Hafner (1969, 1970) and Saxena and Ghose (1971) to examine the Fe^{2+}–Mg distribution of orthopyroxenes quenched from various equilibration temperatures.

Electronic absorption spectra are also sensitive to the site distribution of ferrous iron in orthopyroxene. The spectroscopic features of Fe^{2+} in the $M(1)$ and $M(2)$ sites differ in energy and intensity due to the structural differences between the two sites (Burns, 1970; Runciman et al., 1973; Goldman and Rossman, 1976, 1977). Previous electronic absorption studies of orthopyroxenes have not attempted to provide quantitative site distribution information. The purpose of this study is to establish a method from which a quantitative site distribution can be determined from electronic absorption spectra of single orthopyroxene crystals. The advantages of this method are that (1) it can be used to analyze orthopyroxene crystals in a thin-section in which the textural relationships among the various phases are retained, and (2) it can be used to analyze the site distribution in single orthopyroxene crystals to examine the petrologic implications of compositional zonation.

The method results from correlating the intensity of the absorption bands due to Fe^{2+} in the $M(2)$ site in the electronic spectra with the molar concentration of Fe^{2+} in this site, which is determined from Mössbauer spectra (taken at 77 K) and electron microprobe analysis. A linear correlation between the spectroscopic techniques over the compositional range spanned depends on the constancy of the ratio of the recoil-free fractions for both sites in the Mössbauer spectra and the constancy of molar absorptivity for Fe^{2+} in the $M(2)$ site in the electronic absorption spectra. Virgo and Hafner (1968) and Burnham et al. (1971) indicated that differences in recoil-free fraction for Fe^{2+} between both sites are small and assumed that the ratio is equal to one.

Experimental Methods

The electronic absorption spectra of the bronzite from Bamble, Norway are presented in Goldman and Rossman (1977). Other spectra were obtained on polished, self-supporting (010) and (100) slabs. To obtain the intense band in α near 11,000 cm^{-1} on scale for spectroscopic measurement, the (100) slabs were epoxied onto a glass slide, thinned to less than 0.05 mm and spectroscopically examined. The epoxy was then dissolved in N,N-dimethylformamide, the samples were removed and their thicknesses were determined with a micrometer. The thickness of the eulite used to obtain the β spectrum was determined similarly, except on a (001) orientation. Methods of sample preparation and data reduction have been described in Goldman and Rossman (1977). Specific procedures used for determining the intensity of absorption bands in the orthopyroxene spectra involve first correcting the spectra for the baseline variations and instrumental artifacts. The peak intensity of the $M(2)$ bands are then read from the chart paper in the 10,500 cm^{-1} and 5,000 cm^{-1} regions, and the baseline value is subtracted. The baseline value is established at the minimum absorbance near 4,000 cm^{-1}. For well-polished thin crystals, the baseline near 5,000 cm^{-1} can be obtained by extending a ruled line tangent to the minima near 4,000 cm^{-1} and 7,000 cm^{-1} and

Table 1. Chemical analyses

	1	2	3	4
SiO_2	57.83	52.83	53.30	47.38
TiO_2	–	0.07	0.19	–
Al_2O_3	0.09	2.94	0.23	0.79
MgO	32.86	25.08	19.67	3.83
FeO	9.77	18.82	25.02	48.57
MnO	–	0.17	0.51	–
CaO	0.26	0.44	1.76	0.84
	100.81	100.35	100.68	101.41
Formula proportions (# cations = 4)				
Si	2.00	1.92	2.00	1.98
Al^{IV}	–	0.08	–	0.02
Al^{VI}	–	0.05	0.01	0.02
Ti	–	–	0.01	–
Mg	1.70	1.36	1.10	0.24
Fe	0.28	0.57	0.79	1.70
Mn	–	0.01	0.02	–
Ca	0.01	0.02	0.07	0.04

1: Bronzite, Bamble, Norway; 2: Bronzite, Barton garnet mine, Gore Mountain, New York, CIT #3403; 3: Hypersthene, Summit Rock, Oregon (Kleck, 1970); 4: Eulite (XYZ) Greenland (Virgo and Hafner, 1969)

Analyses 1, 2, and 3 are electron microprobe analyses; analysis 4 is the wet chemical analysis from Virgo and Hafner (1969)

for the α and β polarizations the baseline near 11,000 cm^{-1} is approximated by the line tangent to the minima near 7,000 cm^{-1} and 14,500 cm^{-1}. The intensity of the 11,000 cm^{-1} γ band is obtained by subtracting the value of the absorption minimum near 7,000 cm^{-1} from the peak value of the band. Because this band is both weak and subject to interference from $M(1)$ bands and intervalence charge transfer, it is the least useful analytically. Electron microprobe analyses of samples 1, 2 and 3 (Table 1) have been taken within the area in which the optical spectra were obtained. The chemical analysis of the eulite is given in Virgo and Hafner (1969). Site distributions from 77 K Mössbauer spectra have been determined directly from the area ratios. Heating experiments were conducted in evacuated sealed silica tubes which were quenched in liquid nitrogen when the heating period was completed.

The orientation convention is $\alpha(\mathbf{E}\|\mathbf{b}, \mathbf{b} \sim 8.9\,\text{Å}, \beta(\mathbf{E}\|\mathbf{a}, \mathbf{a} \sim 18\,\text{Å}), \gamma(\mathbf{E}\|\mathbf{c}, \mathbf{c} \sim 5.2\,\text{Å})$ where **E** is the vibration direction of the incident electric vector.

Spectroscopic Considerations

Spin-Allowed Bands

Three spin-allowed electronic transitions arising from Fe^{2+} in the $M(2)$ site have been identified in the spectra of orthopyroxenes. In the case of bronzite ($Fs_{14.0}$)

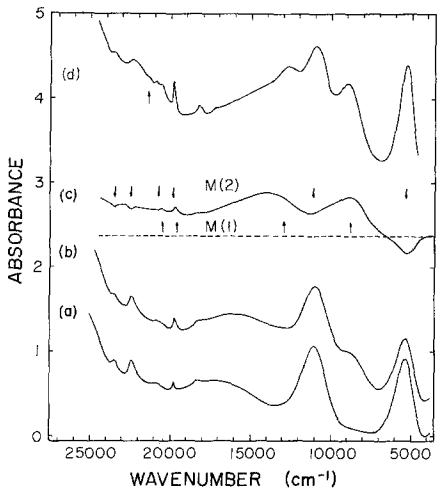

Fig. 1. Room temperature γ electronic absorption spectra of a bronzite from Gore Mountain taken before heat-treatment (**a**) and after heating in a vacuum at 850° C for 24 h (**b**). The unheated spectrum was subtracted from the heated spectrum to produce the difference plot (**c**) in which features due to Fe^{2+} in the $M(1)$ and $M(2)$ sites are denoted by arrows pointing up and down, respectively. The γ spectrum taken at 77 K of a hypersthene from Summit Rock, Oregon (**d**) which was heated in a vacuum at 900 and then 800° C for 48 h clearly shows the two spin-allowed $M(1)$ absorptions near 8,600 and 13,000 cm^{-1}. Spectra (**b**), (**c**), and (**d**) have been displaced vertically for clarity of presentation

from Bamble, Norway, the $^5A_1 \rightarrow {}^5A_1$, $^5A_1 \rightarrow {}^5B_1$ and $^5A_1 \rightarrow {}^5B_2$ transitions occur at 10,930, 5,400, and 2,350 cm^{-1} and are polarized mostly in α, β, and γ, respectively (Goldman and Rossman, 1977). The Mössbauer spectrum of that sample taken at 77 K as a part of the present study indicates that 96.1 % of the iron is in the $M(2)$ site. The transitions to the $^5A_1$ and $^5B_1$ states are considered to originate from a removal of the degeneracy of the octahedral ^5E_g state due to the low symmetry of the site and similarly, the $^5B_2$ state is considered to arise from the splitting of the octahedral $^5T_{2g}$ state.

An absorption band near 8,600 cm^{-1} that is polarized mostly in γ has been assigned to Fe^{2+} in the $M(1)$ site by Burns (1970). Burns considered this band to represent the transition to the lower energy component of the split ^5E_g state. The higher energy component was considered to be beneath the main band in γ due to Fe^{2+} in the $M(2)$ site. To understand the extent to which the $M(1)$ absorptions interfere with the calibrations for the $M(2)$ peak intensities, a series of experiments was performed to identify the location of the higher energy $M(1)$ band. These experiments make use of the ability to disorder the iron distribution between the $M(1)$ and $M(2)$ sites by heating single crystals to temperatures above 500° C and then by quickly quenching the sample. In the course of that study, the origin of the spin-forbidden bands in the 15,000–25,000 cm^{-1} region was also examined.

The γ spectrum of a bronzite ($Fs_{29.5}$) from Gore Mountain is presented in Fig. 1a. The Mössbauer spectrum of this sample taken at 77 K indicates that 94.9 % of the iron is in the $M(2)$ site, and consistent with this result, the intensity of the $M(1)$ band near 8,600 cm^{-1} is weak. The oriented slab used to obtain this spectrum was heated at 850° C for 24 h to disorder Fe^{2+} between the two sites. After heating and quenching, the sample was spectroscopically examined at room temperature (Fig. 1b). The reduction in the intensity of the $M(2)$ feature near 5,400 cm^{-1} and the increase in the intensity of the $M(1)$ feature near 8,600 cm^{-1} verifies the cation disordering phenomenon previously described from Mössbauer spectroscopy (Virgo and Hafner, 1969; Saxena and Ghose, 1971). The absorption tail originating from the ultraviolet region has moved further into the visible region, and the

intensity of the Fe^{2+}/Fe^{3+} intervalence charge-transfer band near 17,000 cm^{-1} (Burns, 1970, p. 72) appears to have increased slightly after heating. Additionally, the transmission valley near 13,500 cm^{-1} (Fig. 1 a) is replaced by absorption after heating (Fig. 1 b), which we attribute to the presence of the higher energy ^5E_g component of Fe^{2+} in the $M(1)$ site. This band becomes evident in a difference plot (Fig. 1 c) in which the unheated spectrum was subtracted from the heated spectrum. The higher energy $M(1)$ band is clearly evident in the 77 K γ spectrum (Fig. 1 d) of a volcanic hypersthene ($Fs_{39.5}$) from Summit Rock, Oregon that has been heated at 900 and then 800° C, each for 48 h. From these observations, the upper ^5E_g component for Fe^{2+} in the $M(1)$ site is estimated to have an energy of 13,000 cm^{-1}, which produces a barycenter (mean) energy of both components of 10,800 cm^{-1}.

Spin-Forbidden Bands

Five narrow bands of low intensity occur in γ at 23,470, 22,400, 20,800, 19,760, and 18,250 cm^{-1} (Fig. 1 a). They are considered to arise from spin-forbidden transitions of Fe^{2+} in the $M(2)$ site because they are prominent in the spectrum of low-iron orthopyroxenes such as sample #1 which contain Fe^{2+} predominantly in the $M(2)$ site. After heating (Fig. 1 b), the bands at 23,470 and 22,400 cm^{-1} have diminished in intensity as shown in the difference plot (Fig. 1 c), supporting their assignment to the $M(2)$ site. After heating, new bands appear at 20,500 and 19,700 cm^{-1} which we attribute to Fe^{2+} in the $M(1)$ site. Problems of overlap make the changes in intensity of the other bands difficult to determine accurately. At greater $M(1)$ concentrations (Fig. 1 d), another band near 21,370 cm^{-1} appears that is attributed to Fe^{2+} in the $M(1)$ site. These assignments differ in detail from those of Langer and Abu-Eid (1977), based on calculated energy level diagrams, although it is agreed that they arise from Fe^{2+} spin-forbidden bands. The most intense Fe^{3+} spin-forbidden band occurs in the range 22,700–23,300 cm^{-1} in monoclinic pyroxenes such as acmite and spodumene. The absence of a band in this range in our spectra indicates that the formation of Fe^{3+} during the heating experiment is not a problem. Our site assignments are summarized in Fig. 1 c in which absorptions due to Fe^{2+} in the $M(1)$ and $M(2)$ sites are annotated with arrows pointing up and down, respectively.

The Calibration

The spectra of the two bronzites and the hypersthene sample form the basis for the calibration of optical intensities. The 77 K Mössbauer spectrum of the hypersthene sample indicates that 82.1 % of the total iron content resides in the $M(2)$ site. The spectrum of the eulite (Fs_{86}) containing nearly full Fe^{2+} occupancy of the $M(2)$ site is also included which has bands at 10,850 and 4,890 cm^{-1}. The cation distribution in this sample was determined by both X-ray and Mössbauer analyses in Burnham et al. (1971).

In order to calculate the concentration of Fe^{2+} in the $M(2)$ site for any sample, the density must be known. It would be particularly advantageous to obtain the

density of a crystal in a thin section without having to extract it. Howie (1963) showed that the density of orthopyroxene regularly increases with increasing iron content. Therefore, an equation can be determined to relate density to iron content, enabling densities to be calculated from electron microprobe analyses of orthopyroxene crystals in a thin-section. From the thirty-eight chemical analyses and density measurements in Howie (1963), two in Deer et al. (1966), and using the density measurement for the Bamble sample in Gibbons (1974), the following least-squares equation is obtained:

$$D(\mathrm{g/l}) = 13.37(\pm 0.02) \times (\mathrm{wt\,\%FeO}) + 3{,}186.13(\pm 0.47) \quad (1)$$

where D is the density in grams per liter and FeO is the total iron content in the sample. The densities of the Gore Mountain and Summit Rock samples were determined from Eq. (1), whereas the density of the Greenland sample was calculated from the chemistry and cell axes given in Burnham et al. (1971). The Fe^{2+} concentration in each site and the intensities of the $M(2)$ electronic absorption features are listed in Table 2.

The intensities of α, β, and γ components of the $^5A_1 \rightarrow {}^5A_1$ and $^5A_1 \rightarrow {}^5B_1$ transitions in the 10,500–11,000 and 4,900–5,400 cm^{-1} regions respectively are correlated with the Fe^{2+} concentrations in the $M(2)$ site (Figs. 2 and 3). All the spectral intensities are linearly related to Fe^{2+} concentration in the range up to 10 mol/l of Fe^{2+} in the $M(2)$ site which represents nearly 66 % occupany of the $M(2)$ site by Fe^{2+}. For eulite, the intensities of both bands in β and the 5,000 cm^{-1} band in α fall close to the linear trend determined by the other samples. The minor departure from the trend of the 11,000 cm^{-1} eulite band in β may be attributed to interference from an $M(1)$ band. A weak component of the 8,600 cm^{-1} $M(1)$ band, dominantly polarized in γ, also occurs in β in this sample. The intensity of the γ

Table 2. Optical intensities[a]

	Sample				
	1	2	3	4	
α	172	347	410	927	10,500–
β	20	44	54	90	11,000 cm^{-1}
γ	8	20	27	[b]	region
α	6	15	16	24	4,900–
β	42	85	99	138	5,400 cm^{-1}
γ	11	20	26	46	region
Fe conc. (mol/l)[c]					
$M(1)$	0.2	0.5	2.2	11.5	
$M(2)$	4.3	8.5	10.0	14.7	

[a] Absorbance per centimeter crystal thickness
[b] Difficult to determine
[c] Data for samples 1, 2, and 3 from Mössbauer spectra; sample 4 from the X-ray data of Virgo and Hafner (1969)

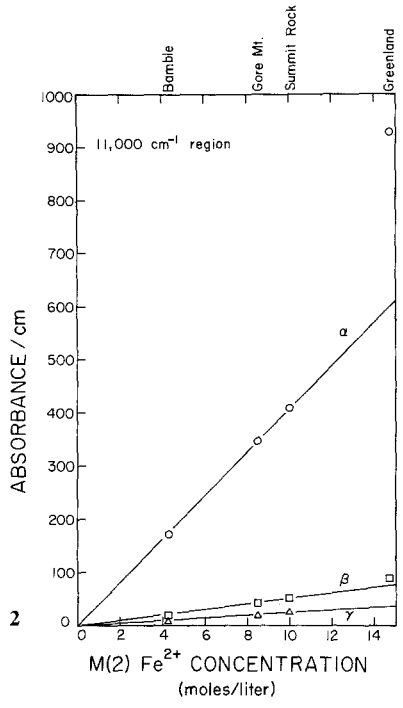

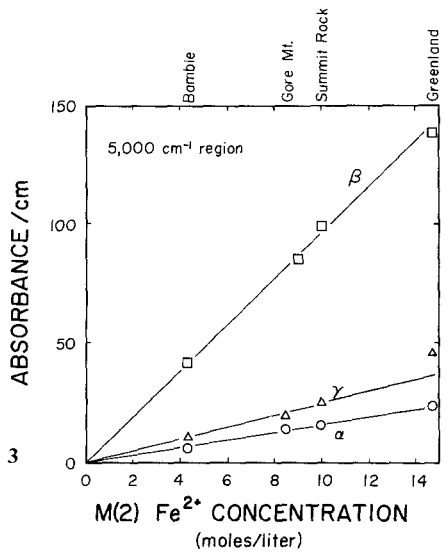

Fig. 2. Correlation of the intensities of the $M(2)$ bands in the 10,500–11,000 cm^{-1} region with the concentration of Fe^{2+} in the $M(2)$ site

Fig. 3. Correlation of the intensities of the $M(2)$ bands in the 4,900–5,400 cm^{-1} region with the concentration of Fe^{2+} in the $M(2)$ site

band of eulite near 11,000 cm^{-1} cannot be readily determined because of problems with extensive overlap of the $M(1)$ features. The eulite band in α near 11,000 cm^{-1}, which has an absorbance per cm value of 927, clearly falls off of the linear trend as does the band in γ near 5,000 cm^{-1}. These deviations have been confirmed with three samples of the Greenland eulite.

Molar absorptivity (ε) values for all bands in the linear regions of Figs. 2 and 3 have been determined from least-squares solutions of the data and are presented in Table 3. From these results, the $M(2)$ iron concentration can be determined from any band using the following:

$$Fe^{2+}_{M(2)}(\text{mol/l}) = Abs/(T \cdot \varepsilon) \tag{2}$$

where Abs is the optical absorbance ($\log I_0/I$), T is the thickness (in centimeters) and ε is the molar absorptivity for that band given in Table 3. Equation (2) can be rewritten to give the iron content in weight percent as:

$$Fe^{2+}_{M(2)}(\text{wt}\%) = \frac{Abs \cdot (5{,}585)}{T \cdot \varepsilon \cdot D} \tag{3}$$

Table 3. Molar absorptivity (ε) for $M(2)$ Fe^{2+}

	α	β	γ
10,500–11,000 cm^{-1}	40.8	5.24	2.51
4,900–5,400 cm^{-1}	1.59	9.65	2.48

where D is the density determined from Eq. (1). To determine the iron content as FeO, replace 5,585 by 7,185 in Eq. (3). The values determined from these equations are then subtracted from the total iron content to obtain the $M(1)$ Fe^{2+} content.

The ε value for the $M(1)$ band near 8,600 cm^{-1} in the γ spectrum of the Summit Rock hypersthene (Goldman and Rossman, 1977, Fig. 3) is calculated to be 4.6. An ε value of 4.7 is calculated for this band from the Gore Mountain bronzite after heating (Fig. 1b) using Eq. (2).

The band in α in the 10,000–11,000 cm^{-1} region is the most sensitive means for determining the cation distribution and is about four times as intense as the band in β in the 5,000–5,500 cm^{-1} region. For a 30 μm thick orthopyroxene crystal which contains 0.5 %FeO, all of which is in the $M(2)$ site, the absorbance in α at about 11,000 cm^{-1} would be about 0.03 which is readily detectible in the spectra. For the Bamble bronzite in a thin section, this indicates that about a 5 % change in the $M(2)$ iron content can be detected at this thickness from the spectra. Similarly, a 2 % change in the $M(2)$ iron content of the Summit Rock hypersthene can be detected. The deviation from linearity at high concentration, most likely a result of geometric changes in the $M(2)$ coordination environment, has not been found to be a problem in actual applications of the calibration curve. For iron rich samples, the 11,000 cm^{-1} α band is too intense at sample thicknesses normally encountered to be useful. Under these conditions, the other, less intense adsorption bands are prefered.

Technical Problems

To make these determinations of cation concentration, it is necessary to determine the thickness of the crystal. When it is in thin section, oriented sections of quartz can be incorporated into the thin-section, and the thickness of the quartz can be determined after polishing using the appropriate refractive index of quartz with the Duc de Chalnes method (Bloss, 1961, p. 48). If a universal stage is used for orientation, the appropriate thickness corrections must be made.

The effect of convergent light is potentially more important than errors in thickness determination as a source of error in quantitative optical absorption measurements. Convergent light, necessarily introduced by microscope optical systems, mixes the polarization components of the various absorption bands.

The effect of convergence in the optical path can be demonstrated for an idealized example in a typical spectroscopic experiment (Fig. 4). A beam of linearly polarized light, with a convergence angle θ, interacts with an oriented crystal in the $\alpha\beta$ plane for which the absorbances per unit thickness are 0.0 and 1.0 in the α and β directions, respectively. The resulting intensity leaving the sample is:

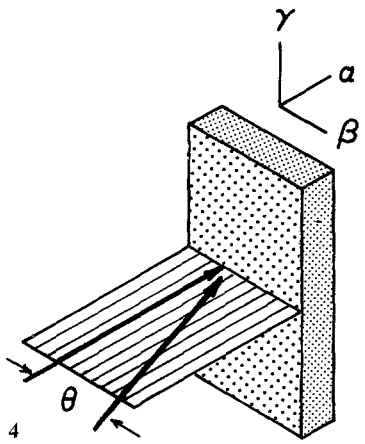

4

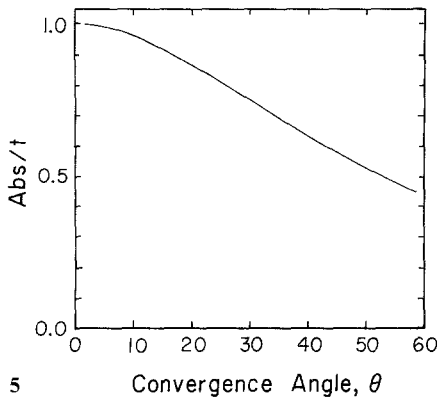

5

Fig. 4. An idealized optical absorption experiment designed to obtain the β spectrum in which plane polarized light with a convergence angle θ interacts with a crystal in both the α and β directions

Fig. 5. The reduction in the intensity of an absorbance band in an idealized optical experiment as a function of the convergence angle, θ

$$I = I_\beta \cos^2\theta + I_\alpha \sin^2\theta. \tag{4}$$

Taking the ratio of this intensity to that in the reference chamber (I_0) in a dual-beam spectrometer results in:

$$Abs/\mathrm{t} = -\log(I/I_0) = -\log[(I_\beta/I_0)\cos^2\theta + (I_\alpha/I_0)\sin^2\theta]. \tag{5}$$

Integrating this equation to account for the total convergence as:

$$2\int_0^\theta 10^{-Abs/\mathrm{t}}\,\mathrm{d}\theta = 2\int_0^\theta \left(\frac{I\beta}{T_0}\right)\cos^2\theta\,\mathrm{d}\theta + 2\int\left(\frac{I\alpha}{I_0}\right)\sin^2\theta\,\mathrm{d}\theta \tag{6}$$

results in

$$Abs/\mathrm{t} = -\log\left\{\frac{1}{2}\frac{\sin\theta\cos\theta}{\theta}\left[\frac{I_\beta}{I_0} - \frac{I_\alpha}{I_0}\right] + \frac{1}{2}\left[\frac{I_\beta}{I_0} + \frac{I_\alpha}{I_0}\right]\right\}. \tag{7}$$

Using Eq. (7), the reduction in the intensity of the β feature as the convergence angle increases is shown in Fig. 5. Therefore, with a 30° convergence angle, the β feature will only be about 75% of its true intensity. The convergence angle in the spectrometer used in this study is less than 3°.

The effects of convergence will be most evident in spectra taken with high power objective lenses on a microscope spectrophotometer, and especially for samples which have a highly absorbing band in one polarization only. The nature of the convergence problem in an actual microscope spectrophotometer will depend upon the properties of the microscope optics and will be more complicated than our idealized example calculation above. These effects result in a lowered

absorption intensity and a flat-topped absorption band which displays characteristics similar to those caused by stray light in spectrophotometers. Many examples of this are to be found in the literature. In some cases, the flat-topped absorption has been fit to two or more gaussian components when the effects of stray light and convergent light have not been recognized.

Conclusion

The correlation of band intensity with the concentration of Fe^{2+} in the $M(2)$ site enables quantitative cation distributions to be determined from electronic spectra and microprobe analyses for single orthopyroxene crystals. Site populations can now be determined for orthopyroxene crystals in petrographic thin-section without sacrificing important textural relationships among the coexisting phases. This technique may be particularly useful in studying the site distribution in zoned or partially exsolved orthopyroxene crystals.

Acknowledgements. We thank J. Huneke (Caltech) and S. Ghose (University of Washington) for providing the hypersthene and eulite crystals used in this study. We also thank Wayne A. Dollase (University of California, Los Angeles) for obtaining the 77 K Mössbauer spectra. A portion of this study was funded by the National Science Foundation, Grant EAR 76-02014.

References

Bloss, F.D.: An Introduction to the Methods of Optical Crystalography. New York: Holt Rinehart and Winston 1961

Burnham, C.W., Ohashi, Y., Hafner, S.S., Virgo, D.: Cation distribution and atomic thermal vibrations in an iron-rich orthopyroxene. Am. Mineral. **56**, 850–875 (1971)

Burns, R.G.: Mineralogical Applications of Crystal Field Theory. Cambridge: Cambridge University Press 1970

Deer, W.A., Howie, R.A., Zussman, J.: An Introduction to the Rock-Forming Minerals. New York: John Wiley and Sons 1966

Evans, B.J., Ghose, S., Hafner, S.S.: Hyperfine splitting of Fe^{57} and Mg-Fe order-disorder in orthopyroxene ($MgSiO_3 - FeSiO_3$) solid solution. J. Geol. **75**, 306–322 (1967)

Ghose, S.: $Mg^{2+} - Fe^{2+}$ order in an orthopyroxene, $Mg_{0.93}Fe_{1.07}Si_2O_6$. Z. Krist. **122**, 81–99 (1965)

Ghose, S., Hafner, S.: $Mg^{2+} - Fe^{2+}$ distribution in metamorphic and volcanic orthopyroxenes. Z. Krist. **125**, 157–162 (1967)

Gibbons, R.V.: Experimental effects of high shock pressure on materials of geologic and geophysical interest. Ph. D. Thesis. California Institute of Technology (1974)

Goldman, D.S., Rossman, G.R.: Identification of a mid-infrared electronic absorption band of Fe^{2+} in the distorted M(2) site of orthopyroxene, $(Mg, Fe)SiO_3$. Chem. Phys. Lett. **41** (3), 474–475 (1976)

Goldman, D.S., Rossman, G.R.: The spectra of iron in orthopyroxene revisited: The splitting of the ground state. Am. Mineral. **62**, 151–157 (1977)

Howie, R.A.: Cell parameters of orthopyroxenes. Mineral. Soc. Am. Spec. Paper **1**, 213–222 (1963)

Kleck, W.C.: Cavity minerals at Summit Rock, Oregon. Am. Mineral. **55**, 1396–1404 (1970)

Langer, K., Abu-Eid, R.M.: Measurements of the polarized absorption spectra of synthetic transition metal-bearing silicate microcrystals in the spectral range 44,000–4,000 cm^{-1}. Phys. Chem. Minerals **1**, 273–299 (1977)

Runciman, W.A., Sengupta, D., Marshall, M.: The polarized spectra of iron in silicates. I Enstatite. Am. Mineral. **58**, 444–450 (1973)

Saxena, S.K., Ghose, S.: $Mg^{2+} - Fe^{2+}$ order-disorder and the thermodynamics of the orthopyroxene crystalline solution. Am. Mineral. **56**, 532–559 (1971)
Virgo, D., Hafner, S.S.: Re-evaluation of the cation distribution in orthopyroxenes by the Mössbauer effect. Earth Planet Sci. Lett. **4**, 265–269 (1968)
Virgo, D., Hafner, S.S.: Fe^{2+}, Mg order-disorder in heated orthopyroxenes. Mineral. Soc. Am. Spec. Paper **2**, 67–81 (1969)
Virgo, D., Hafner, S.S.: Fe^{2+}, Mg order-disorder in natural orthopyroxenes. Am. Mineral. **55**, 201–223 (1970)

Received April 14, 1978